Autophagy Plays a Critical Role in the Degradation of Active RHOA, the Control of Cell Cytokinesis, and Genomic Stability

Amine Belaid[1,3,10], Michaël Cerezo[1,3,4], Abderrahman Chargui[1,3,10], Elisabeth Corcelle–Termeau[11], Florence Pedeutour[1,3,5,6], Sandy Giuliano[3,4], Marius Ilie[1,3,5,7,10], Isabelle Rubera[3,8], Michel Tauc[3,8], Sophie Barale[2,3], Corinne Bertolotto[3,4], Patrick Brest[1,3,10], Valérie Vouret-Craviari[1,3,10], Daniel J. Klionsky[12], Georges F. Carle[2,3], Paul Hofman[1,3,5,7,9,10], and Baharia Mograbi[1,3,10]

Abstract

Degradation of signaling proteins is one of the most powerful tumor-suppressive mechanisms by which a cell can control its own growth. Here, we identify RHOA as the molecular target by which autophagy maintains genomic stability. Specifically, inhibition of autophagosome degradation by the loss of the v-ATPase *a3* (*TCIRG1*) subunit is sufficient to induce aneuploidy. Underlying this phenotype, active RHOA is sequestered via p62 (SQSTM1) within autolysosomes and fails to localize to the plasma membrane or to the spindle midbody. Conversely, inhibition of autophagosome formation by *ATG5* shRNA dramatically increases localization of active RHOA at the midbody, followed by diffusion to the flanking zones. As a result, all of the approaches we examined that compromise autophagy (irrespective of the defect: autophagosome formation, sequestration, or degradation) drive cytokinesis failure, multinucleation, and aneuploidy, processes that directly have an impact upon cancer progression. Consistently, we report a positive correlation between autophagy defects and the higher expression of RHOA in human lung carcinoma. We therefore propose that autophagy may act, in part, as a safeguard mechanism that degrades and thereby maintains the appropriate level of active RHOA at the midbody for faithful completion of cytokinesis and genome inheritance. *Cancer Res; 73(14); 4311–22. ©2013 AACR.*

Introduction

Cells are faced with the tasks of dividing, of keeping the genome intact, and even of dying when appropriate. At their heart, these cell fates are dictated by tumor suppressor mechanisms. One such mechanism is autophagy, which is commonly mutated or downregulated in human cancers (1). Indeed, the essential autophagy gene *BECN1* is deleted or mutated in 40% to 75% of breast, ovarian, colon, and prostate cancers. Consistently, the notion that autophagy suppresses tumor development came from the demonstration that allelic loss of *Becn1* predisposes mice to lymphomas, hepatocellular carcinomas, and lung carcinomas (2, 3). Likewise, defects in other autophagy genes (*Atg4c*, *Atg5*, *Uvrag*, *Ambra1*, and *Bif-1/Sh3glb1*) render cells or mice tumor prone (4–8).

Physiologically, autophagy ensures in all cell types the turnover of all organelles and most long-lived proteins by a pathway, which begins with the formation of a double-membrane compartment, termed a "phagophore" that sequesters them. The phagophore expands into a completed vesicle, an "autophagosome," and subsequently, the autophagosome rapidly fuses with a lysosome to become an "autolysosome" where the content is finally degraded. Originally identified as a housekeeping process, emerging data suggest that constitutive autophagy (i.e., under nutrient-rich conditions) might also fight cancer by limiting inflammation (9), facilitating senescence (10), or clearing signaling proteins (11). Likewise, recent studies reveal that both BECN1 and ATG5 function as "guardians" of cellular genome. Epithelial cells with loss of *Becn1* or *Atg5* display gene amplification and aneuploidy (7, 8). In support, activation of autophagy was shown to reduce genomic instability within hepatocarcinoma cells (12). However, despite the importance of aneuploidy in cancer development (13, 14), the mechanisms underlying how autophagy deficiency compromises genomic stability are still unknown.

To address this issue, we explored the possibility that signaling proteins essential for cell growth might be degraded by autophagy. Whereas significant advances have been made in the discovery of autophagy machinery, less is known about the nature of the autophagy substrates. Therefore, a key feature of our strategy was to inhibit the autophagy pathway at the

Authors' Affiliations: [1]Institute of Research on Cancer and Ageing of Nice (IRCAN), INSERM U1081, CNRS UMR7284, [2]Laboratoire TIRO-MATOs UMR E4320, Commissariat à l'Energie Atomique, Centre Antoine Lacassagne; [3]Université de Nice-Sophia Antipolis, Faculté de Médecine; [4]INSERM U895/C3M; [5]Centre Hospitalier Universitaire de Nice, Pasteur Hospital; [6]Laboratory of Solid Tumors Genetics; [7]Laboratory of Clinical and Experimental Pathology; [8]TIANP, UMR 6097; [9]Human Biobank, Nice; [10]Equipe Labellisée par l'ARC, Villejuif, France; [11]Cell Death and Metabolism Unit, Danish Cancer Society Research Center, Copenhagen, Denmark; and [12]University of Michigan, Life Sciences Institute, Ann Arbor, Michigan

Note: Supplementary data for this article are available at Cancer Research Online (http://cancerres.aacrjournals.org/).

Corresponding Author: Baharia Mograbi, Institute of Research on Cancer and Ageing of Nice (IRCAN); Centre Antoine Lacassagne, Avenue de Valombrose; 06107 Nice Cedex 02, France. Phone: 334-92031245; Fax: 334-92031241; E-mail: mograbi@unice.fr

doi: 10.1158/0008-5472.CAN-12-4142

degradation step, to achieve sequestration and accumulation of substrates within autolysosomal structures (Supplementary Fig. S1A).

Materials and Methods

Cell culture and treatments

To inhibit the maturation of autophagosomes into degradative autolysosomes, renal cells derived from proximal convoluted tubules of wild-type (WT, $a3^{+/+}$) or the lysosomal v-ATPase *a3/TCIRG1*-null mice ($a3^{-/-}$) were isolated and immortalized with the pSV3 neo vector. The renal epithelial cell lines that do or do not express *a3* were referred to as WT and $a3^{-/-}$ cells, respectively. As controls, cells were stimulated with an inhibitor of v-ATPase activity, bafilomycin A1 (100 nmol/L, bafA1; Sigma); or a weak base that raises intralysosomal pH, chloroquine (100 μmol/L, CQ; Sigma). Alternatively, the formation of autophagosomes was inhibited at the initiation step by *Atg5* or *Atg7* short hairpin RNA (shRNA). As a further control, we analyzed the phenotype of *Atg5* KO MEFs (provided by N. Mizushima; ref. 15) and *ATG5*-depleted A549 lung epithelial cells. We also prevented the sequestration of autophagy substrates within the autophagic vesicles by *p62* shRNA. For details on cell culture and shRNA sequences, see Supplementary Information.

Clinical samples

Primary non–small cell lung cancer (NSCLC; pairs of pathologic and control tissues from the same patient) were obtained from patients in Nice (France) and collected by the Tumor Biobank of Nice Hospital (Nice CHU, agreement 2010–06).

Analysis of autophagy

The activity of the autophagy pathway was monitored by 4 hallmarks: (i) the formation of autophagic vesicles; and the degradation of 3 well-established autophagy substrates: (ii) membrane-associated LC3-II, (iii) p62/SQSTM1, and (iv) long-lived proteins.

Ploidy determination and chromosomal abnormalities by metaphase spread

At 70% confluency, cells were arrested with colchicine (Invitrogen) in metaphase. Chromosomes were stained with Giemsa, and about 150 mitotic figures per cell line were photographed and the number of chromosomes was counted by Metafer M-Search Metaphase Finder and Ikaros softwares (Metasystems).

Time lapse video microscopy

For monitoring cell progression through mitosis, exponentially growing cells cultured in complete growth medium were imaged every 5 minutes during 18 hours on an inverted microscope (Carl Zeiss) equipped with a CO_2-equilibrated chamber.

Analysis of the RHOA pathway

The activity of RHOA pathway was monitored by (i) the levels of active GTP-bound RHO (RHOTEKIN RHO-binding domain pull-down and ELISA-based G-LISA assays, Cytoskeleton Inc.), (ii) the recruitment of RHOA to membranes, and (iii) the downstream phosphorylation of myosin regulatory light chain (P-MLC) and reticulation of actin cytoskeleton.

RHOA immunoprecipitation

Cells were lysed in radioimmunoprecipitation assay (RIPA) and RHOA was immunoprecipitated with anti-RHOA antibody (clone 26C4; Santa-Cruz Biotechnology) followed by Western blotting with anti-ubiquitin, anti-p62, anti-LC3, and anti-RHOA antibodies.

RHOA stability

HEK 293 cells and A549 cells (control, *ATG5*, or *p62* shRNA-transduced cells) were transfected with FuGene^{HD} (Promega) and plasmids encoding the active (RHOA Q63) or inactive (RHOA N19) RHOA mutants. Twenty hours after transfection, cells were treated with cycloheximide (CHX; Sigma; C-4859; 10–20 μg/mL) to stop *de novo* protein synthesis for 7 to 57 hours, alone or in combination with proteasomal (MG132, Sigma; 10 μmol/L) and lysosomal (CQ; 100 μmol/L) inhibitors, and the drop in the levels of RHOA mutants was assayed by anti-myc Western blotting (Millipore; P01106; 1:1,000).

Complete and detailed description of all methods used is available as Supplementary Data.

Statistical analysis

When adequate, results are presented as means ± SD from the indicated number n of separate experiments. Statistical comparisons were done using χ^2 or Student t tests as appropriate. $P < 0.05$ was considered significant.

Results

The V-ATPase a3-dependent autophagy defect is characterized by the formation of giant multinucleate cells

To gain a deeper insight into the role of autophagy, we established cell lines from v-ATPase *a3/TCIRG1*-null mice (16). PCT (proximal convoluted tubule) cells were chosen as they express the highest level of v-ATPase (17); the a3 subunit is localized in the lysosomal limiting membrane (18). In agreement with the other reported defect of v-ATPase (19, 20), we show that the *a3* loss increased autophagy sequestration and simultaneously impaired autophagic degradation, as evidenced by the accumulation of ATG12–ATG5 conjugate, of autolysosomes and of autophagic substrates (long-lived proteins, LC3-II, and p62; Fig. 1A and Supplementary Fig. S1B). In contrast, *a3*-null cells seemed to have functionally intact proteasomes (Supplementary Fig. S1C). Remarkably, this a3-dependent autophagy defect was characterized by an increase in cell size and a flattened morphology with the accumulation of vesicles and nuclei (Fig. 1B and C), supporting the importance of autophagy in maintaining cell size (21, 22).

By using different approaches, we excluded a role for senescence as a cause of enlarged morphology (Supplementary Fig. S2). Consistently, fluorescence-activated cell-sorting (FACS) analysis revealed that $a3^{-/-}$ cells were dividing and displayed

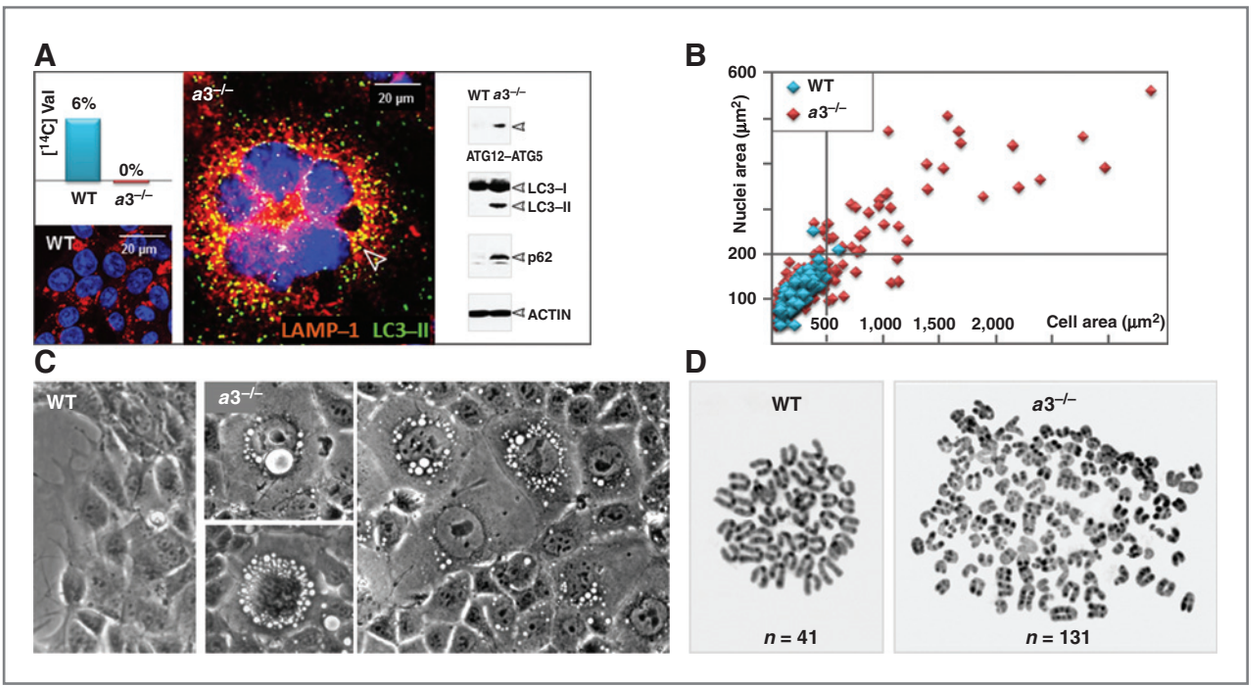

Figure 1. The a3-dependent autophagy defect is characterized by the formation of giant multinucleate cells. A, accumulation of autolysosomes (LC3-II and LAMP1 positive; fluorescence images) that were defective in the degradation of long-lived proteins (top left inset), LC3-II and p62 (right insets). Right, note the accumulation of the ATG12–ATG5 conjugate (a marker of autophagosome formation) in response to the *a3* loss (see Supplementary Fig. S1). B, cell and nuclei area of WT and $a3^{-/-}$ cells ($n = 400$). C, representative photomicrographs showing that the WT cells were all small (200 ± 47 μm^2) with one nucleus, whereas the *a3*-null cells were heterogeneous in size. About 30% to 40% of $a3^{-/-}$ cells showed a gigantic size (200–7,300 μm^2) and a flattened shape with the accumulation of vesicles and nuclei. D, representative karyotype figures showing aneuploidy and structural abnormalities in $a3^{-/-}$ cells.

increased DNA content (3–4 N; Supplementary Fig. S2C). Of interest, no subdiploid or subtetraploid cells were detected, indicating that the *a3* loss did not induce cell death. Subsequent karyotypes of $a3^{-/-}$ cells confirmed a near-triploid karyotype (group average, 131; Fig. 1D). Therefore, despite aneuploidy, the $a3^{-/-}$ cells continued to proliferate and escaped apoptosis or senescence. All these abnormalities, which are hallmarks of cancer cells, were reminiscent of that reported for $Atg5^{-/-}$ or $Becn1^{-/+}$ cells (8). Collectively, these data support the notion that defects of the entire autophagy pathway [i.e., either at the step of formation ($Atg5^{-/-}$ or $Becn1^{-/+}$) or degradation (herein, *V-ATPase* $a3^{-/-}$) of autophagosomes] could result in aneuploidy.

The multinucleate phenotype of $a3^{-/-}$ cells arises from cytokinesis failure

We hypothesized that the aneuploidy of $a3^{-/-}$ cells might arise through cytokinesis failure. Multiple mitotic defects leading to aneuploidy were indeed identified in $a3^{-/-}$ cells, as these cells often showed multipolar spindles and several chromosome segregation defects: improper attachment of chromosomes to spindle microtubules, lagging chromosomes, chromosome bridges connecting daughter cells, and micronuclei. Strikingly, a large proportion of $a3^{-/-}$ cells were connected via an asymmetric bridge, in contrast to the short intracellular bridge observed in the middle of the two WT daughter cells (Supplementary Fig. S3).

Using real-time imaging, we showed that the WT cells completed cytokinesis in only 15 min (Fig. 2A, Supplementary Movie S1). In contrast, the cytokinesis was incomplete upon v-ATPase inhibition by bafilomycin A1 treatment (Fig. 2B) or *a3* loss (Fig. 2C–G, Supplementary Movies S2–S5). About 72% of $a3^{-/-}$ cells that entered mitosis normally failed abscission (Fig. 2C) and instead remained connected by an intracellular bridge for up to 8 hours before separating (Fig. 2D, Supplementary Movie S2), re-entering mitosis synchronously (still bound to the sister cell, Fig. 2E, Supplementary Movie S3) or collapsing back, forming a single binucleate cell (Fig. 2F and G, Supplementary Movies S4 and S5). Moreover, we did not observe cell–cell fusion, cell engulfment, and endoreplication during live cell imaging ($n = 200$). Thus, impairment of cytokinesis at the membrane abscission step was the key event responsible for the formation of multinucleate $a3^{-/-}$ cells.

The inhibition of autophagy degradation by v-ATPase *a3* loss stabilizes RHOA-GTP within autolysosomes

We then explored which signaling proteins might be degraded by autophagy and could underlie this phenotype. One candidate was the small GTPase RHOA that dictates cell shape and completion of cytokinesis via F-actin reticulation (23). In this regard, a striking hallmark of $a3^{-/-}$ cells was a dramatic remodeling of actin cytoskeleton with the loss of stress fibers and the formation of actin patches (Fig. 3A and Supplementary Fig. S4A and S4B). The current consensus is that fine-tuning of

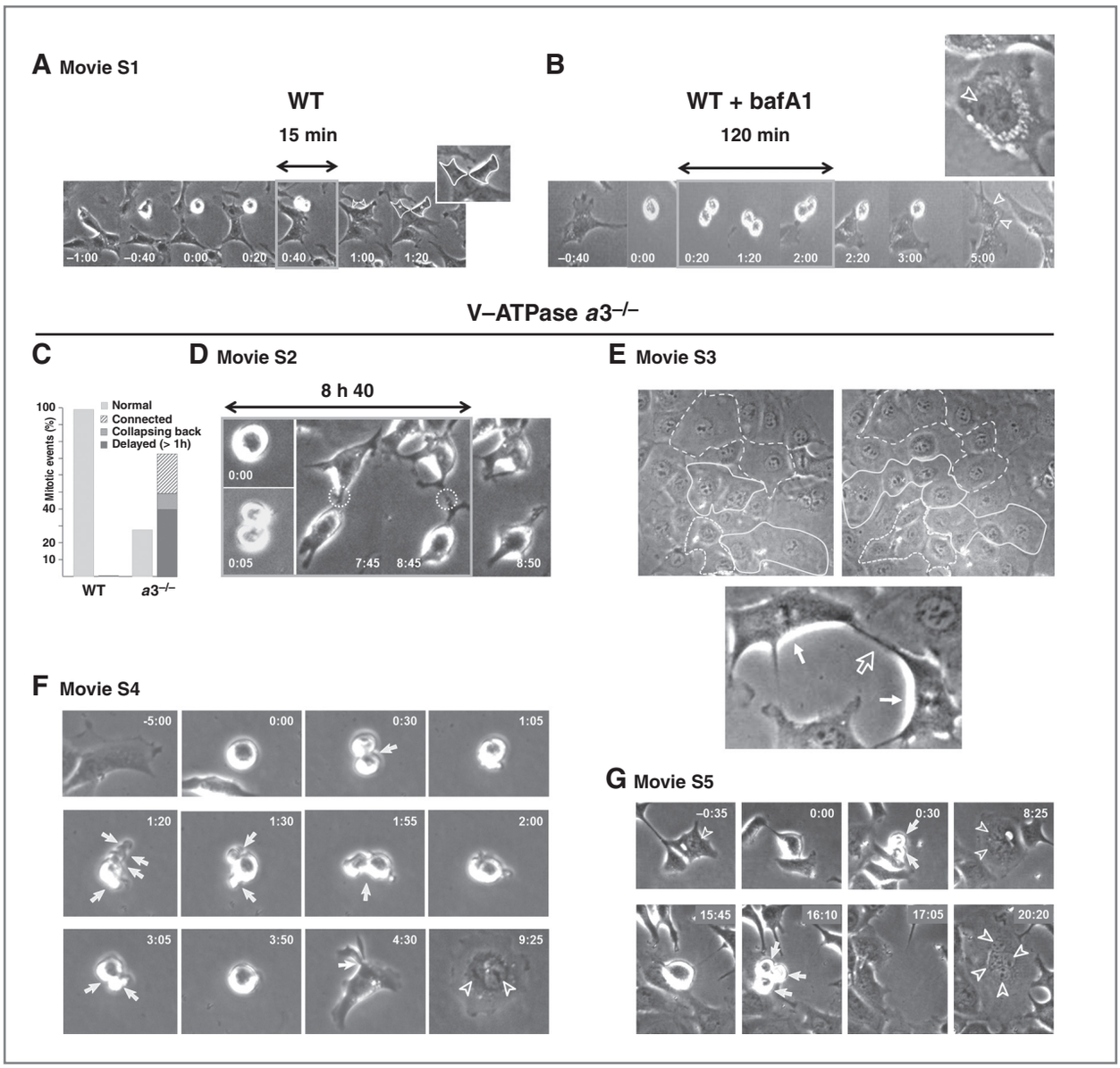

Figure 2. Cytokinesis is specifically impeded by v-ATPase inactivation. Control (A, treated with dimethyl sulfoxide, Supplementary Movie S1; inset, high magnification of the last frame where the daughter WT cells are outlined in white to help visualize their successful division), bafA1-treated WT cells (B, 100 nmol/L, 8 hours after the addition of bafA1), or $a3^{-/-}$ cells (C–G, Supplementary Movies S2–S5), all under complete medium, were followed for 18 hours using phase-contrast time lapse microscopy. C, frequency of cytokinesis failure in $a3^{-/-}$ cells ($n = 125$). D, still images of a mitotic $a3^{-/-}$ cell that remained connected by an intracellular bridge for up to 8 hours before abscission (Supplementary Movie S2). E, pairs of $a3^{-/-}$ cells that entered mitosis synchronously are outlined in white (Supplementary Movie S3). Bottom, 2 mitotic cells (white arrows) remained connected by an intracellular bridge (empty arrow). F, still images of an $a3^{-/-}$ cell that exited mitosis as a binucleated cell after 18 attempts of cleavage furrow formation. Note that this cell developed ectopic furrows, which led to the formation of anuclear fragments (white filled arrows) that fused back to the cell (Supplementary Movie S4). G, still images of a mononucleate $a3^{-/-}$ cell that formed a tetranucleate cell after 2 rounds of abortive mitoses (Supplementary Movie S5). Both giant and small $a3^{-/-}$ cells failed cytokinesis, resulting in multinucleation and differentially sized daughter cells. All daughter cells were viable throughout imaging (up to 18 hours). White empty arrows indicate cleavage furrow formation, arrowheads indicate nuclei, and time points are in hours:minutes from the initiation of metaphase (zero time point).

RHO activity involves the guanine nucleotide exchange factors (GEF) that activate them, the GTPase-activating proteins (GAP) that inactivate them, and the guanine nucleotide dissociation inhibitors (GDIs) that maintain RHO inactive within the cytoplasm (23). Exciting findings have revealed that RHO GTPases, their upstream regulators and downstream targets might also be subjected to irreversible proteasome-dependent degradation (24–32).

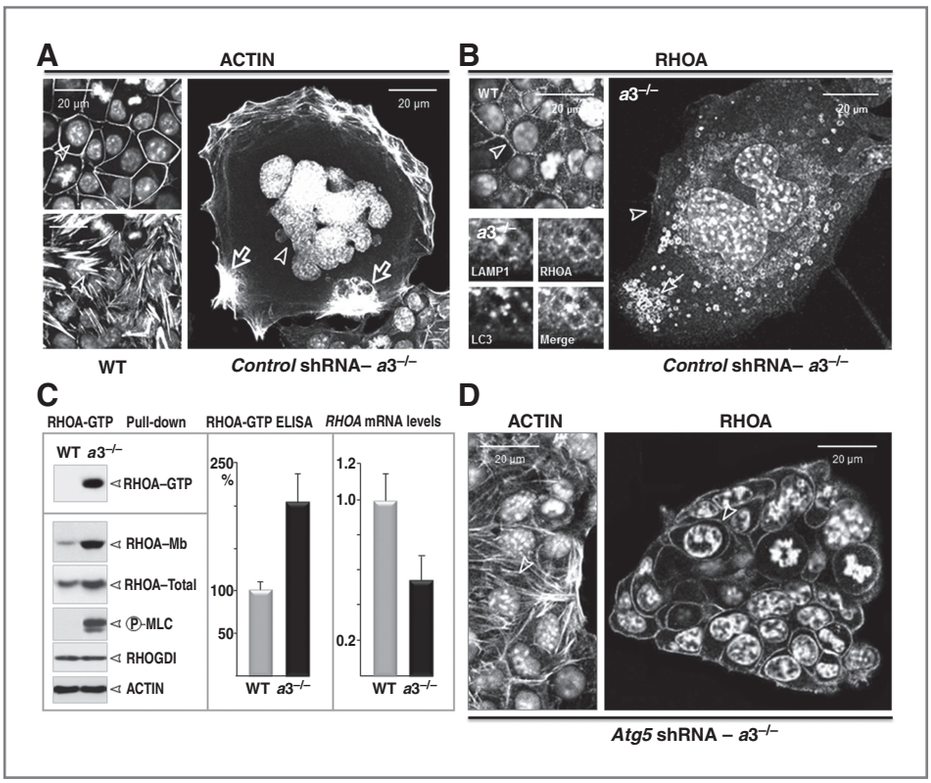

Figure 3. The inhibition of autophagy degradation by v-ATPase *a3* loss stabilizes RHOA-GTP within autolysosomes. A, phalloidin labeling showed the loss of stress fibers in $a3^{-/-}$ cells that instead developed actin patches (empty arrows). B, intracellular ring of RHOA (arrows) that colocalized with LC3-II and LAMP1 (insets; see also the color images in Supplementary Fig. S4B, left) in $a3^{-/-}$ cells in contrast to the WT cells that displayed RHOA at their plasma membrane (arrowhead). C, accumulation of RHOA-GTP in $a3^{-/-}$ cells was evidenced by RHOTEKIN binding (pull-down assay and G-ELISA kit; left and middle, respectively); the recruitment of active RHOA proteins to Triton X-100 insoluble cell membranes; and the downstream phosphorylation of myosin regulatory light chain (Ⓟ-MLC; bottom). Bound proteins (top) and total cell lysates (bottom) were analyzed by Western blotting. Note that *a3* loss increased the ratio of activated (membrane-associated): total RHOA from 2% (WT) to 4% ($a3^{-/-}$ cells). Western blot analyses are representative of 3 independent experiments. Reverse transcriptase PCR analysis showing that RHOA-GTP accumulation was not due to an increased *RHOA* transcription (right). D, *Atg5* shRNA rescues RHOA localization at the plasma membrane (arrowhead) of $a3^{-/-}$ cells. Cells were infected with *Atg5* shRNA lentivirus and selected with media containing puromycin for 72 hours. Shown are representative images where 4′,6-diamidino-2-phenylindole (DAPI) marks nucleus and F-actin denotes the filamentous actin stained by phalloidin.

Instead of proteasome, however, we determined that active RHOA was constitutively maintained at low levels by autophagy. Indeed, the active RHOA was barely detected at the plasma membrane of $a3^{-/-}$ cells but instead accumulated intracellularly within autolysosomes positive both for the autophagy marker LC3 and lysosomal marker LAMP1 (Fig. 3B, Supplementary Fig. S4B, inset). Notably, the level of RHOA-GTP was elevated in resting $a3^{-/-}$ cells, as evidenced by the RHOTEKIN-binding pull-down assay, the recruitment of RHOA to cellular membranes and the downstream phosphorylation of myosin regulatory light chain (P-MLC; Fig. 3C, Supplementary Fig. S4B).

A role for autophagy in controlling RHOA-GTP level was then suggested by the shRNA-mediated inhibition of autophagosome formation: Expression of *Atg5* shRNA increased the localization of active RHOA at the plasma membrane of $a3^{-/-}$ cells, which allowed actin polymerization into filaments (Fig. 3D). Consistently, the *Atg5* shRNA-transduced $a3^{-/-}$ cells displayed a smaller size and tight cohesion within the colony (Fig. 3D). Importantly, the control of RHOA by autophagy was remarkably specific, as the related GTPase RAC (Supplementary Fig. S4E), as well as the RHOA regulator, RHOGDI, were not affected (Fig. 3C). Together, these data highly suggest a working model in which autophagy might sequester and degrade active RHOA. Inhibition of v-ATPase by *a3* loss would stabilize RHOA-GTP within autolysosomal structures, protecting it from autophagy degradation, and at the same time, this would preclude reticulation of actin cytoskeleton (Supplementary Fig. S1A).

p62-dependent autophagy specifically degrades active RHOA

As proof-of-concept, pharmacologic inhibition of autophagy degradation by bafA1 or CQ treatment similarly increased the levels of membrane-bound RHOA together with the autophagy substrates LC3-II and p62 (Supplementary Fig. S5). This occurred in multiple cell types including fibroblast, kidney, and lung epithelial cells (Supplementary Fig. S5A). In contrast, impairment of proteasome by MG132 failed to alter the levels of the membrane-bound RHOA in every cell line

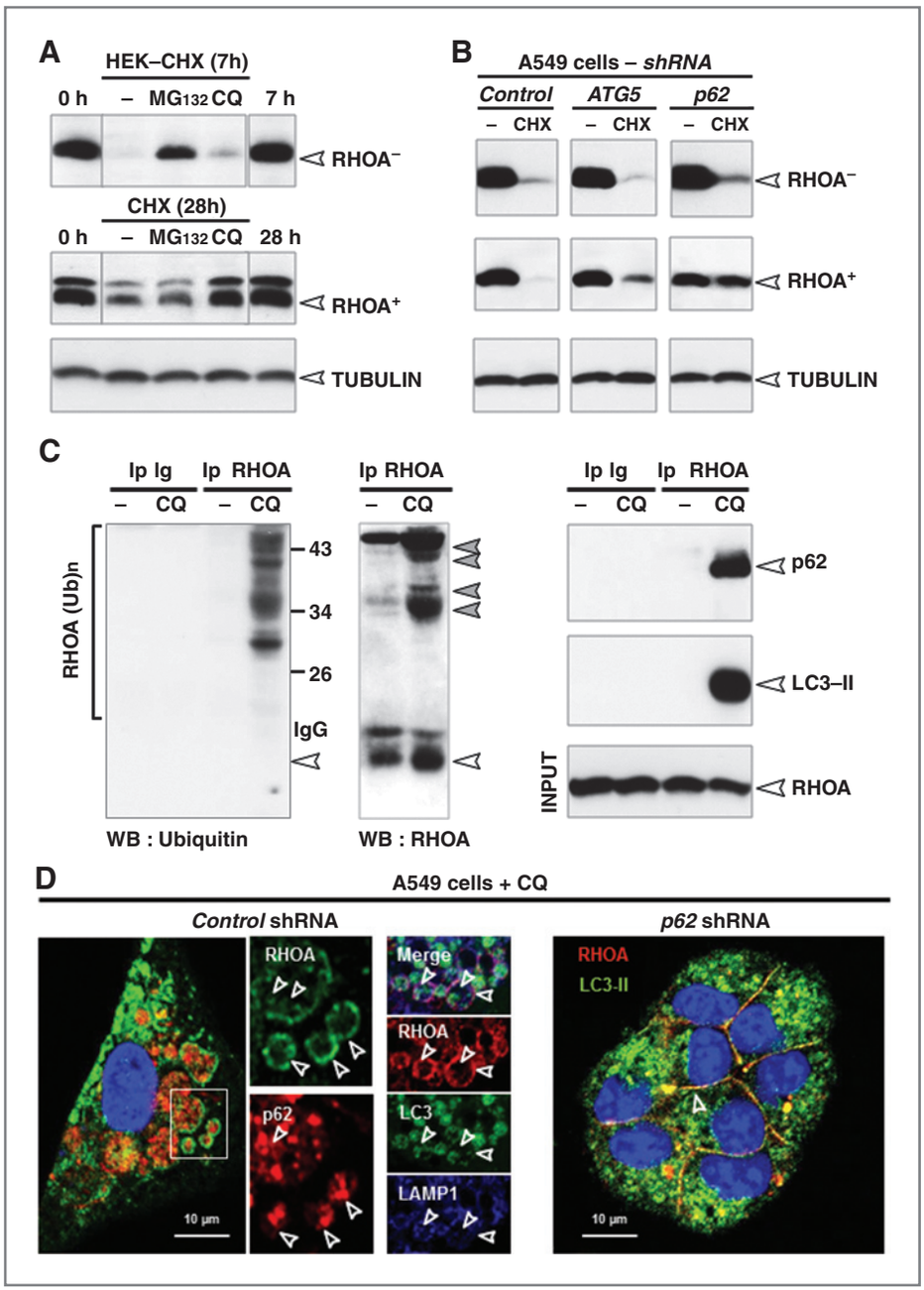

Figure 4. p62-dependent autophagy controls the levels of active RHOA. A, the active RHOA is specifically degraded by a lysosomal pathway. HEK cells were transfected with plasmids encoding the active (Q63, RHOA^{+}) or inactive RHOA (N19, RHOA^{-}) mutants and incubated with CHX (10 μg/mL) for the indicated time in the presence or absence of CQ (100 μmol/L) or MG132 (10 μmol/L) to inhibit the lysosomal or proteasomal functions, respectively. Expression of RHOA mutants was analyzed by anti-myc Western blotting (see Supplementary Fig. S5). B, inhibiting autophagy sequestration in A549 cells by *ATG5* or *p62* depletion stabilized the active but not the inactive RHOA mutant. Control, *ATG5*, or *p62* shRNA-transduced A549 cells were transfected with the RHOA mutants and treated with CHX (20 μg/mL) for 57 hours. Equal protein loading was verified by anti-tubulin immunoblotting. The data are representative of at least 3 independent experiments (see Supplementary Fig. S6A and S6B). C, the ubiquitin-binding protein p62/SQSTM1 acts as a receptor that targets the active RHOA to autophagy. Ubiquitinated RHOA species (gray arrowheads) formed a complex with p62 and LC3-II in CQ-treated A549 cells. D, p62 affects RHOA localization. Left, RHOA colocalized with p62, LC3-II, and LAMP1 upon autophagy inhibition by CQ; right, decreasing p62 levels by shRNA reduced colocalization of RHOA with LC3-II and rescued RHOA localization at the plasma membrane of CQ-treated cells.

tested (Supplementary Fig. S5A). As expected, all features of $a3^{-/-}$ cells (i.e., RHOA autolysosomal recruitment, F-actin depolymerization, and increased cell size) were mimicked by bafA1, but not MG132 treatment, further supporting the model that activity of the RHOA pathway can be controlled by the autophagy–lysosome pathway (Supplementary Fig. S5B and S5C). Consistently, the active, but not inactive, RHOA mutants were long-lived proteins selectively degraded by autophagy (Fig. 4). Indeed, upon inhibition of protein synthesis with cycloheximide, the active RHOA (RHOA^{+}, Q63) was degraded within 28 hours and stabilized by inhibiting lysosomal degradation (CQ, Fig. 4A), or autophagosome formation (*ATG5* shRNA, Fig. 4B and Supplementary Fig. S6A and S6B) but not proteasomal activity (MG132, Fig. 4A). Inversely, the inactive form of RHOA (RHOA^{-}, N19) was unstable and as expected stabilized by inhibition of proteasome but not by inhibition of lysosomal activity or of autophagy (Fig. 4A and B), in agreement with previous reports (24–30).

At this stage, it was of interest to address how autophagy may specifically target the active RHOA. One adaptor by which autophagy acquires specificity is p62 (SQSTM1) that targets ubiquitinated substrates to the autophagy machinery

(33). Of interest, p62 appears as a prime candidate for regulating RHOA as it is the sole autophagy adaptor involved in cell mitosis (34), cell spreading (35), and tumor growth (36–38). We observed that p62 not only co-immunoprecipitated (Fig. 4C) and co-localized (Fig. 4D) with ubiquitinated RHOA and LC3-II in CQ-treated cells but was also essential in the selective clearance of active RHOA by autophagy (Fig. 4B and D). Upon p62 silencing and CQ treatment, autophagosomes formed normally (as evidenced by LC3-II conversion, Supplementary Fig. S6A), but the autophagic sequestration (Fig. 4D) and degradation (Fig. 4B) of active RHOA were defective. Collectively, these results strongly suggest a new signaling role for p62-dependent autophagy in the control of RHOA pathway.

Regulation of the amount of active RHOA at the midbody during cytokinesis by autophagy

The multinucleate phenotype of $a3^{-/-}$ cells raised the question of whether autophagy may control cytokinesis through regulation of RHOA. Autophagy was suggested to clear the midbody ring after cytokinesis completion (39, 40). Likewise, the depletion of several autophagy genes (*Atg5*, *Becn1*, *Uvrag*, *Bif-1*, And *Vps34*) was shown to lead to polynucleation, but the role of autophagy in controlling RHOA activation during cytokinesis was not documented (8, 41).

Although several key RHOA activators have been identified (42), little is known about the mechanisms that confine active RHOA at the midbody. Using the $a3^{-/-}$ cells, we observe that little, if any, active RHOA was at the equatorial furrow and was instead sequestered within autolysosomes, close to the midbody (Fig. 5A), likely as a result of increased sequestration. Inversely, when we blocked autophagosome formation by *ATG5* shRNA (Supplementary Fig. S6A), RHOA was highly enriched at the equatorial furrow of cytokinetic A549 lung cancer cells (Fig. 5B, Supplementary Fig. S7A). Notably, the RHO activity zone in *ATG5*-depleted cells was 3 times as wide and bright as in controls (control shRNA $= 3.7 \pm 0.8$ μm; *ATG5* shRNA $= 11.4 \pm 2.6$ μm; mean $\pm$ SD; Fig. 5C and D). Outside the cell equator, RHOA activity was also abnormally high at the cell cortex (Fig. 5B, Supplementary Fig. S7). Accordingly, *Atg5* knockdown in mouse embryonic fibroblasts (Fig. 5E) and *ATG7* or *p62* depletion in A549 cells (Supplementary Fig. S6) faithfully recapitulated the same phenotype with regard to the RHOA pathway. Likewise, closer examination indicated that the upstream regulators required for narrowed activation of RHOA such as the kinesin MKLP1, the RHOA GEF ECT2, and spindle microtubules concentrated at the midbody of cytokinetic cells (Supplementary Fig. S8A and S8B; ref. 43). It is also highly likely that the loss of *ATG5* would create defects in the generation and the delivery of new membranes to the cleavage furrow, a process that is central to cytokinesis. As shown in Supplementary Fig. S8C, the delivery of endosomes to the midbody appeared not to be affected by *ATG5* depletion: the endosomes were delivered to the cleavage furrow and clustered on either side of midbody of *ATG5*-depleted cells, as observed in control cells. In contrast, *ATG5*-depleted cells exhibited in addition to RHOA a broader distribution of downstream F-actin that triggers the formation of actomyosin ring (Supplementary Fig. S7B). Our data therefore suggest that the degradation of RHOA by autophagy may function as a key, but hitherto uncharacterized, mechanism concentrating active RHOA at midbody.

Autophagy defects fuel chromosomal instability in lung cancer cells

Considering the apparent connection between autophagy and RHOA, a key issue is how defects in autophagy might affect cell behavior in a way relevant for cancer progression. Maintaining the appropriate amount of active RHOA at midbody is critical for faithful cytokinesis as it dictates the position, the formation and the contraction of actomyosin ring (42, 44). If our model were correct, one would expect that the inhibition of autophagy sequestration in autophagy-competent A549 tumor cells would be sufficient to disturb cytokinesis and thereby drive the genomic instability required for tumor progression. As shown in Fig. 6, in control A549 cells, the clustering of RHOA in a narrow zone resulted in the formation of a unique and compact ring whose position and size remained constant throughout furrow ingression (Fig. 6A and B, top). As a result, control cells successfully completed cytokinesis (Supplementary Movie S6). Without functional autophagy, the subsequent hyperactivation of RHOA zone would jeopardize the assembly of an efficient contractile ring, as expected from the cytokinesis defects observed for active RHOA mutants (Supplementary Fig. S4C). Indeed, *ATG5*-depleted A549 cells progressed through mitosis until the furrow started to constrict, then 52% of the cells showed unstable and loose furrowing that suddenly fell apart, reformed, and constricted more slowly than control furrows, delaying cytokinesis completion (Fig. 6A and B, bottom, Supplementary Movie S6). As result of cytokinesis failure, these autophagy compromises (*ATG5* shRNA and *p62* shRNA) were sufficient to increase the percentage of cells with multiple nuclei (Fig. 6C), and the frequency of chromosomal gains and losses in nearly all of the chromosomes (Fig. 6D), one hallmark of aggressive cancers. Together, these findings highly suggested that autophagy may act, in part, as a master safeguard mechanism of active RHOA localization during cytokinesis for faithful genome inheritance.

Overexpression of RHOA is correlated with autophagy defects in lung carcinomas

The biochemical, cellular, and genomic changes (increased RHOA activity, increased cellular sizes, and aneuploidy) we consistently observed herein following autophagy inhibition (irrespective of particular autophagy defects) are noteworthy because they accompany the onset and progression of cancers. RHOA overexpression has been observed in many aggressive cancers, such as breast, colon, prostate, and lung cancers, but has been attributed largely to increased *RHOA* transcription (45). Consistent with a role of autophagy in RHOA degradation, we found that RHOA, together with p62 and LC3-II, were overexpressed in late stages of NSCLCs (T; pTNM stage IIIA), compared with normal epithelia (N) and stage I adenocarcinomas (Fig. 7A and B). An impaired autophagic degradation rather than an increased transcription was correlated with RHOA overexpression, as the levels of RHOA expression and activity increased progressively with the accumulation of the autophagy substrates p62 and LC3-II (Fig. 7A), and no

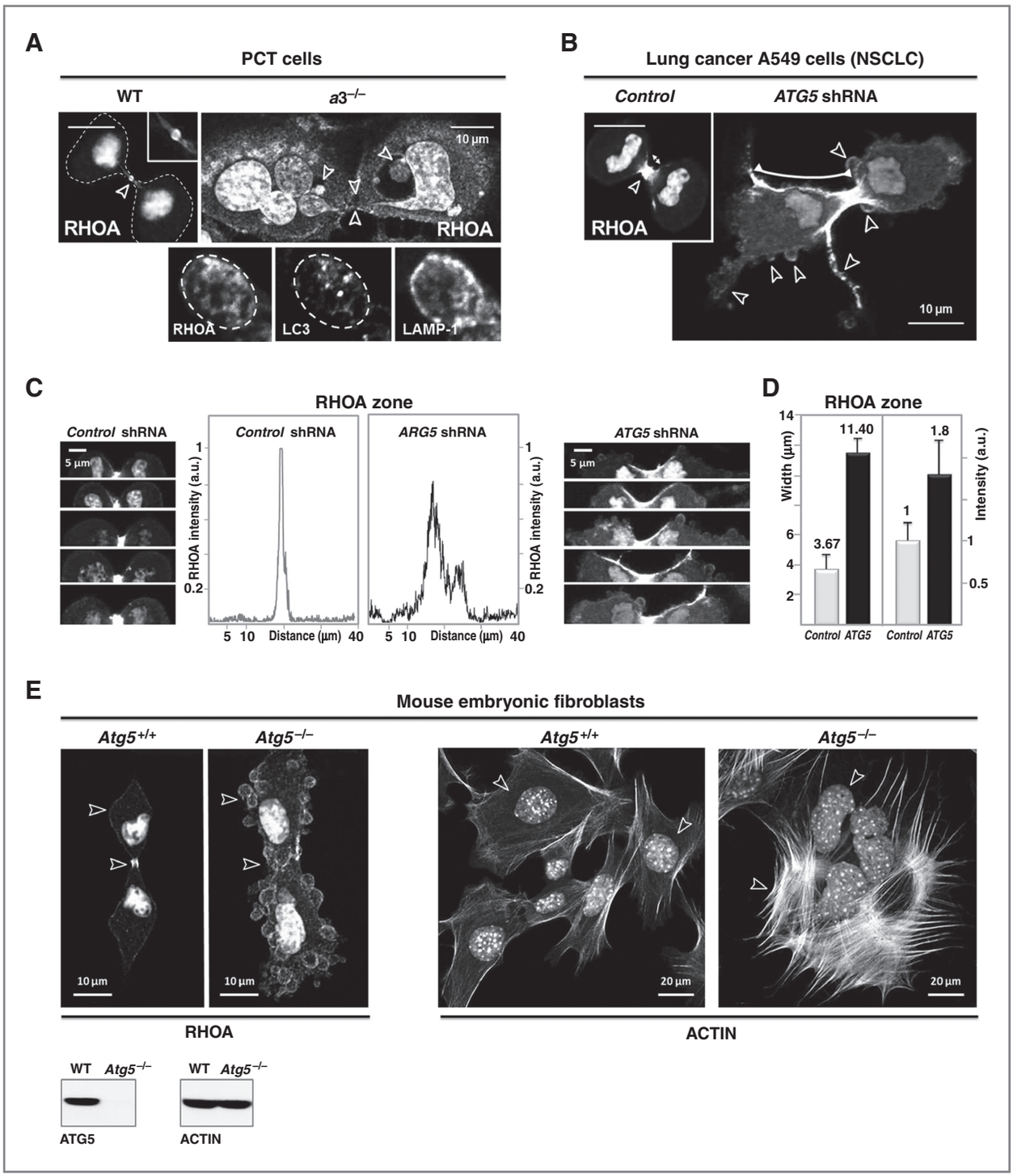

Figure 5. Autophagy defects disturb the clustering of active RHOA at the midbody during cytokinesis. A, confocal images of cytokinetic $a3^{-/-}$ PCT cells showing that RHOA failed to localize to midbody (arrowhead) and instead accumulated within autolysosomes (LC3 and LAMP1 positive). Inset, RHOA-positive vesicles were not degraded and accumulated within the luminal space of autolysosomes. B, *ATG5* depletion in A549 tumor cells caused aberrant RHOA diffusion along the cell cortex during cytokinesis. RHOA, normally detected in a narrow zone at midbody of control cells, accumulated within a looser equatorial zone (arrows) and outside (arrowheads) of cleavage furrow of *ATG5*-depleted cells (see Supplementary Figs. S6A and S7). C, RHOA staining at similar stages of furrowing in control (left) and *ATG5*-depleted (right) A549 cells. Representative intensity profile that measures RHOA zone width along the cell edge (middle). D, the increases in the RHOA zone width ($P = 5.34 \times 10^{-8}$) and RHOA intensity (area under curve, $P = 0.000266995$) reflect a net increase in RHOA activation at equatorial region of *ATG5*-depleted cells. Results are mean ± SD; $n = 15$. E, compared with WT cells, $Atg5^{-/-}$ MEF cells showed severe RHOA diffusion over the entire cell surface, ectopic furrowing during cytokinesis, as well as enlarged nuclei and cell morphology, and enhanced F-actin polymerization.

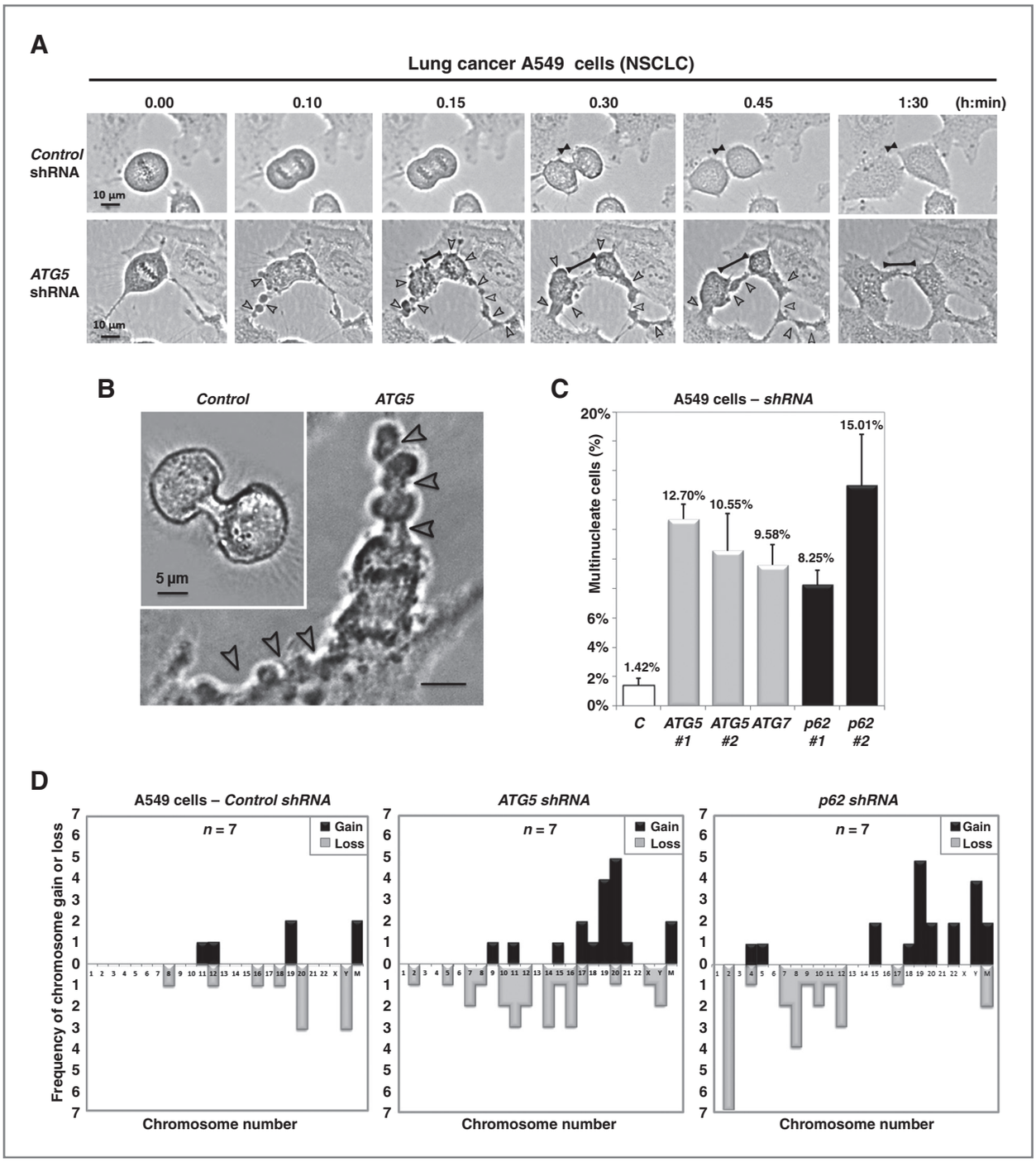

Figure 6. Autophagy defects cause genomic instability in lung cancer cells. A, persistent ectopic furrowing as *ATG5*-depleted A549 cells entered cytokinesis. Phase-contrast images of control and *ATG5*-depleted A549 cells were acquired at the indicated times (hours:minutes; Supplementary Movie S6). Virtually all control cells showed normal compact furrowing during cytokinesis (85%; $n = 100$, top inset), whereas the majority (52%; $P = 2.8 \times 10^{-19}$; $n = 50$) of telophase *ATG5*-depleted cells exhibited unstable and loose furrowing. The black arrowheads indicate ectopic furrows and the bar marks the width of the equatorial furrow. B, representative picture of a telophase *ATG5*-depleted cell that exhibited unstable furrowing, with numerous cortical constrictions and blebs (arrowheads), in contrast to the unique and compact furrow of a control cell (see Supplementary Fig. S7). C, defects at the stage of autophagosome formation (*ATG5* or *ATG7* shRNA) or the recruitment of autophagy substrates (*p62 shRNA*) resulted in a 7- to 10-fold increase of multinucleate cells compared with control shRNA-transduced cells. The different autophagy defects are indicated on the *x*-axis ($n = 900$). The *y*-axis shows the percentage of multinucleate cells (see Supplementary Fig. S6C). D, frequency of whole chromosome gains (black) and losses (gray) in control, *ATG5*-depleted, and *p62*-depleted A549 cells ($n = 7$). Chromosome numbers are indicated on the *x*-axis. Note that the chromosomal gains or losses occurred with low frequency in the autophagy-competent A549 tumor cells and were limited to fewer chromosomes in comparison with *ATG5*-depleted cells and *p62*-depleted cells, which showed widespread chromosomal gains and losses in nearly all of the chromosomes. Chromosome 2 loss ($n = 7$) and chromosome 19 gain ($n = 5$) were recurrent in *p62*-depleted A549 cells.

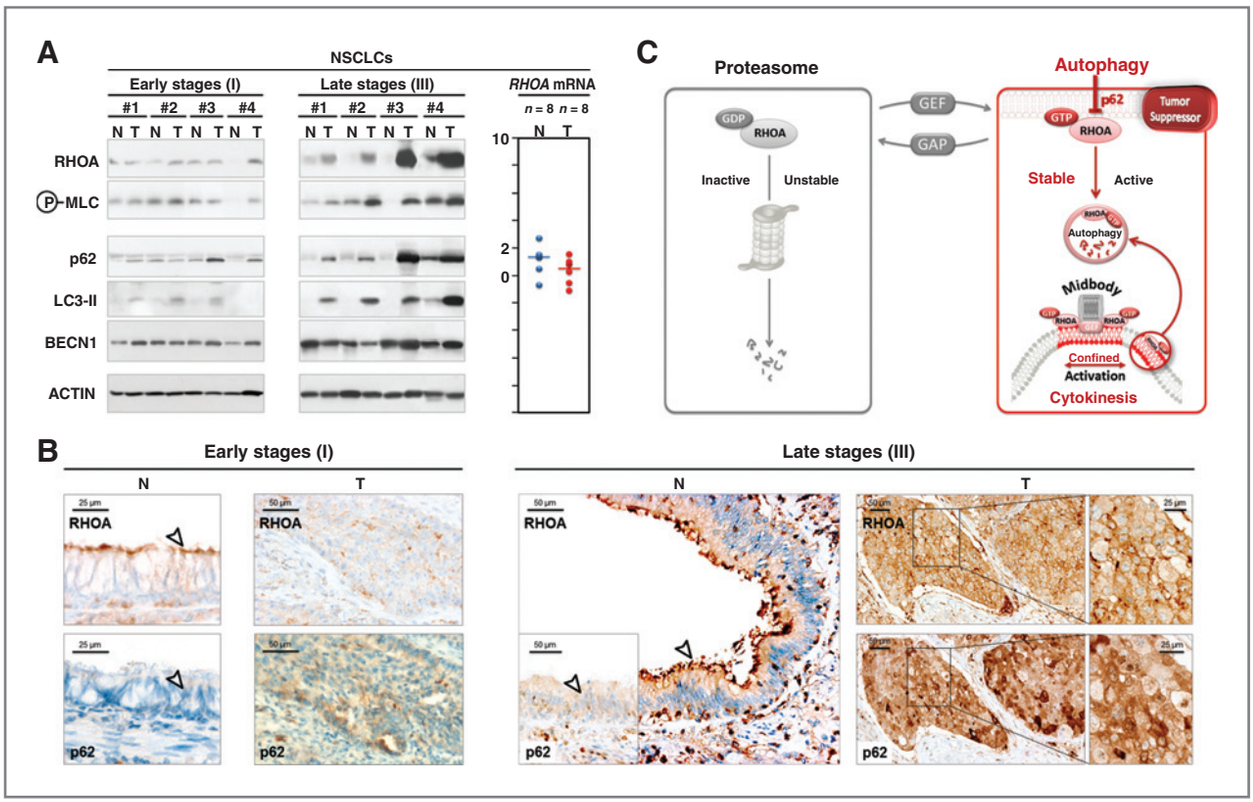

Figure 7. Correlation between RHOA protein levels and autophagy in human lung cancers. A, immunoblotting of NSCLC samples (T, tumor: early stage $n = 4$; late stage $n = 4$; see Supplementary Table S1) versus normal peritumoral tissues (N, normal) using the indicated antibodies. p62 served as a positive control for autophagy impairment (36) and actin as a loading control. Similar *RHOA* mRNA levels in tumor and normal tissues (right, not statistically significant). B, immunohistochemical staining revealed a high overexpression of RHOA and p62 in late stages of NSCLCs. In line with $a3^{-/-}$ cell results (Fig. 3), the defect in lung cancer samples was a defect in autophagosome degradation with the concomitant accumulation of the 3 autophagy substrates LC3, p62, and active RHOA (RHOA recruitment to intracellular cell membranes; and downstream Ⓟ-MLC). C, proposed model by which autophagy sequesters and degrades the active RHOA that would otherwise diffuse from midbody to flanking zones. Together with RHO GEF, autophagy seems essential to confine RHOA activation at midbody, allowing the assembly of a unique and compact contractile ring, for successful cytokinesis and faithful genome inheritance.

significant changes in *RHOA* mRNA expression were measured (Fig. 7A, right). Of interest, the inactivation of autophagy and the subsequent RHOA upregulation were not early events but instead were late events in the progression of lung cancer, when these cancers acquire a more genomic instability. All tumor cells positive for p62 were also RHOA-positive (Fig. 7B). p62 overexpression, as a readout of an autophagy defect, was associated with a reduced or absent RHOA membrane localization, which instead displayed intracellular localization (T, right). In sharp contrast, normal bronchial epithelial cells that barely expressed p62 showed strong membrane expression of RHOA primarily at their apical ciliated cell surface (N, left).

Discussion

So far, most studies suggest that signal termination and irreversible progression through cell cycle depend largely on the proteasomal degradation of key regulatory proteins (46). Recently, Gao and colleagues provide the first evidence that autophagy negatively regulates Wnt signaling by degrading Dishevelled; however, this occurs under nutrient starvation (11). Therefore, the ability of autophagy to degrade signaling proteins under basal conditions and thereby to ensure tumor-suppressive functions remains to be established.

We show here that autophagy promotes the degradation of active RHOA. In support of this, (i) RHOA-GTP was elevated in cells deficient in autophagosome clearance, (ii) importantly, RHOA failed to localize to midbody and instead accumulated within autolysosomes, (iii) a role for autophagy in regulating RHOA-GTP was then suggested by the shRNA-mediated inhibition of autophagosome formation: *ATG5* shRNA dramatically increased the localization of RHOA-GTP at the equatorial furrow of cytokinetic cells. One related RHO GTPase, RAC, was not targeted by autophagy. As a result, defects of the entire autophagy pathway [i.e., either at the formation (*ATG5* or *ATG7 shRNA*), sequestration (*p62 shRNA*), or degradation of autophagosomes (v-ATPase $a3^{-/-}$ cells)] similarly drive the formation of unstable and loose furrowing, disturbing cytokinesis completion and genome inheritance; processes that directly contribute to cancer development.

The regulation of RHOA is unique in that it involves GEF, GAP, and GDI proteins, along with the proteasome (47) and autophagy. Depending on its activation state, we provide the first lines of evidence that RHOA used distinct routes for

degradation: while the proteasome degraded the cytosolic and inactive forms, the autophagy pathway specifically degraded the membrane-associated and active pool of RHOA. This is consistent with the recently reported degradation of 2 constitutively active RHO, RHOH and RHOB, within lysosomes (48, 49) and the redistribution of active RHOA to undefined perinuclear localization after treatment of enterocytes with an autophagy inducer, lipopolysaccharide (LPS; ref. 50). We therefore propose that autophagy may act as a tumor suppressor pathway, in part, by turning off RHOA activation (Fig. 7C). In this model, the remarkable dynamics of autophagy together with its integration of extracellular cues might dictate the time and place where a RHOA is active and is able to interact with its downstream substrates. Accordingly, we reported the targeting of autolysosomes at midbody during cytokinesis, the same subcellular and temporal localizations where RHOA should be controlled. Therefore, autophagy might be critical for localized degradation of active RHOA at midbody and thereby proper actin dynamics during accurate completion of cytokinesis and faithful genome inheritance.

The development of a cancer depends on the ability of tumor cells to acquire growth advantages. Whatever the mutations, deletions, and epigenetic silencing of autophagy genes, our findings provide new information on how autophagy defects can drive tumor progression through deregulation of RHOA pathway. As autophagy is commonly downregulated in cancers (1) where RHOA is overexpressed (47), this new paradigm may be a general mechanism for the acquisition of aneuploidy and progression of human cancer cells.

Disclosure of Potential Conflicts of Interest

No potential conflicts of interest were disclosed.

Authors' Contributions

Conception and design: A. Belaid, B. Mograbi
Development of methodology: A. Belaid, M. Cerezo, B. Mograbi
Acquisition of data (provided animals, acquired and managed patients, provided facilities, etc.): A. Belaid, A. Chargui, F. Pedeutour, S. Giuliano, M. Ilie, I. Rubera, M. Tauc, S. Barale, C. Bertolotto, G.F. Carle, B. Mograbi
Analysis and interpretation of data (e.g., statistical analysis, biostatistics, computational analysis): A. Belaid, A. Chargui, B. Mograbi
Writing, review, and/or revision of the manuscript: M. Ilie, V. Vouret-Craviari, D.J. Klionsky, G.F. Carle, B. Mograbi
Administrative, technical, or material support (i.e., reporting or organizing data, constructing databases): E. Corcelle-Termeau, M. Ilie, P. Brest, P. Hofman, B. Mograbi
Study supervision: B. Mograbi

Acknowledgments

The authors thank Nathalie Rochet, Nathalie Singer, Etienne Boulter, Jean Albrengues, and Emmanuel Lemichez for helpful discussions; Laurence Cailleteau, Thibault Fabas, Annie-Claude Peyron, Valérie Pierrefite-Carle, Isabelle Mothe, Adrien Botta, and Virginie Tanga-Gavric for their technical assistance; and Prof. Mouroux and Prof. Vénissac (Thoracic Surgery Department, Nice, France) and Dr. N. Mizushima (Tokyo, Japan) for providing us with surgical lung specimens and *Atg5* KO MEFs, respectively.

Grant Support

This work was supported by grants from "Institut National de la Santé et de la Recherche Médicale", "Agence de l'Environnement et de la Maîtrise de l'Energie" (A. Belaid and A. Chargui: ADEME n° 0862C0044), Agence régionale santé Provence Alpes Côte d'Azur and Direction régionale de l'Environnement, de l'aménagement et du logement (A. Belaid: plan régional santé environment PRSE PACA n°6.3.3.3 et 6.3.3.4), "Association pour la Recherche contre le Cancer" (ARC Grants no SL220110603478), "Programme Hospitalier De Recherche Clinique" (P. Hofman: PHRC Nice CHU 2003), "Cancéropole PACA" (PROCAN 2007, axe II), "Institut National du Cancer" (P. Hofman: PNES POUMON INCa), and NIH (D.J. Klionsky: GM053396).

The costs of publication of this article were defrayed in part by the payment of page charges. This article must therefore be hereby marked *advertisement* in accordance with 18 U.S.C. Section 1734 solely to indicate this fact.

Received November 9, 2012; revised April 1, 2013; accepted April 1, 2013; published OnlineFirst May 23, 2013.

References

1. Mathew R, Karantza-Wadsworth V, White E. Role of autophagy in cancer. Nat Rev Cancer 2007;7:961–7.
2. Qu X, Yu J, Bhagat G, Furuya N, Hibshoosh H, Troxel A, et al. Promotion of tumorigenesis by heterozygous disruption of the beclin 1 autophagy gene. J Clin Invest 2003;112:1809–20.
3. Yue Z, Jin S, Yang C, Levine AJ, Heintz N. Beclin 1, an autophagy gene essential for early embryonic development, is a haploinsufficient tumor suppressor. Proc Natl Acad Sci U S A 2003;100:15077–82.
4. Fimia GM, Stoykova A, Romagnoli A, Giunta L, Di Bartolomeo S, Nardacci R, et al. Ambra1 regulates autophagy and development of the nervous system. Nature 2007;447:1121–5.
5. Takahashi Y, Coppola D, Matsushita N, Cualing HD, Sun M, Sato Y, et al. Bif-1 interacts with Beclin 1 through UVRAG and regulates autophagy and tumorigenesis. Nat Cell Biol 2007;9:1142–51.
6. Mariño G, Salvador-Montoliu N, Fueyo A, Knecht E, Mizushima N, Lopez-Otin C. Tissue-specific autophagy alterations and increased tumorigenesis in mice deficient in Atg4C/autophagin-3. J Biol Chem 2007;282:18573–83.
7. Karantza-Wadsworth V, Patel S, Kravchuk O, Chen G, Mathew R, Jin S, et al. Autophagy mitigates metabolic stress and genome damage in mammary tumorigenesis. Genes Dev 2007;21:1621–35.
8. Mathew R, Kongara S, Beaudoin B, Karp CM, Bray K, Degenhardt K, et al. Autophagy suppresses tumor progression by limiting chromosomal instability. Genes Dev 2007;21:1367–81.
9. Degenhardt K, Mathew R, Beaudoin B, Bray K, Anderson D, Chen G, et al. Autophagy promotes tumor cell survival and restricts necrosis, inflammation, and tumorigenesis. Cancer Cell 2006;10:51–64.
10. Young AR, Narita M, Ferreira M, Kirschner K, Sadaie M, Darot JF, et al. Autophagy mediates the mitotic senescence transition. Genes Dev 2009;23:798–803.
11. Gao C, Cao W, Bao L, Zuo W, Xie G, Cai T, et al. Autophagy negatively regulates Wnt signalling by promoting Dishevelled degradation. Nat Cell Biol 2010;12:781–90.
12. Xie R, Wang F, McKeehan WL, Liu L. Autophagy enhanced by microtubule- and mitochondrion-associated MAP1S suppresses genome instability and hepatocarcinogenesis. Cancer Res 2011;71:7537–46.
13. Geigl JB, Obenauf AC, Schwarzbraun T, Speicher MR. Defining 'chromosomal instability'. Trends Genet 2008;24:64–9.
14. Fujiwara T, Bandi M, Nitta M, Ivanova EV, Bronson RT, Pellman D. Cytokinesis failure generating tetraploids promotes tumorigenesis in p53-null cells. Nature 2005;437:1043–7.
15. Kuma A, Hatano M, Matsui M, Yamamoto A, Nakaya H, Yoshimori T, et al. The role of autophagy during the early neonatal starvation period. Nature 2004;432:1032–6.
16. Scimeca JC, Franchi A, Trojani C, Parrinello H, Grosgeorge J, Robert C, et al. The gene encoding the mouse homologue of the human osteoclast-specific 116-kDa V-ATPase subunit bears a deletion in osteosclerotic (oc/oc) mutants. Bone 2000;26:207–13.
17. Hurtado-Lorenzo A, Skinner M, El Annan J, Futai M, Sun-Wada GH, Bourgoin S, et al. V-ATPase interacts with ARNO and Arf6 in early endosomes and regulates the protein degradative pathway. Nat Cell Biol 2006;8:124–36.
18. Toyomura T, Murata Y, Yamamoto A, Oka T, Sun-Wada GH, Wada Y, et al. From lysosomes to plasma membrane: localization of vacuolar

type H+-ATPase with the a3 isoform during osteoclast differentiation. J Biol Chem 2003;278:22023–30.
19. Lee JH, Yu WH, Kumar A, Lee S, Mohan PS, Peterhoff CM, et al. Lysosomal proteolysis and autophagy require presenilin 1 and are disrupted by Alzheimer-related PS1 mutations. Cell 2010;141: 1146–58.
20. Juhasz G. Interpretation of bafilomycin, pH neutralizing or protease inhibitor treatments in autophagic flux experiments: novel considerations. Autophagy 2012;8:1875–6.
21. Hosokawa N, Harab Y, Mizushima N. Generation of cell lines with tetracycline-regulated autophagy and a role for autophagy in controlling cell size. FEBS Lett 2006;580:2623–9.
22. Lum JJ, Bauer DE, Kong M, Harris MH, Li C, Lindsten T, et al. Growth factor regulation of autophagy and cell survival in the absence of apoptosis. Cell 2005;120:237–48.
23. Jaffe AB, Hall A. RHO GTPases: biochemistry and biology. Annu Rev Cell Dev Biol 2005;21:247–69.
24. Doye A, Mettouchi A, Bossis G, Clément R, Buisson-Touati C, Flatau G, et al. CNF1 exploits the ubiquitin-proteasome machinery to restrict RHO GTPase activation for bacterial host cell invasion. Cell 2002; 111:553–64.
25. Wang HR, Zhang Y, Ozdamar B, Ogunjimi AA, Alexandrova E, Thomsen GH, et al. Regulation of cell polarity and protrusion formation by targeting RHOA for degradation. Science 2003;302:1775–9.
26. Ozdamar B, Bose R, Barrios-Rodiles M, Wang HR, Zhang Y, Wrana JL. Regulation of the polarity protein Par6 by TGFβ receptors controls epithelial cell plasticity. Science 2005;307:1603–9.
27. Chen Y, Yang Z, Meng M, Zhao Y, Dong N, Yan H, et al. Cullin mediates degradation of RHOA through evolutionarily conserved BTB adaptors to control actin cytoskeleton structure and cell movement. Mol Cell 2009;35:841–55.
28. Bryan B, Cai Y, Wrighton K, Wu G, Feng XH, Liu M. Ubiquitination of RHOA by Smurf1 promotes neurite outgrowth. FEBS Lett 2005;579: 1015–9.
29. Asanuma K, Yanagida-Asanuma E, Faul C, Tomino Y, Kim K, Mundel P. Synaptopodin orchestrates actin organization and cell motility via regulation of RHOA signalling. Nat Cell Biol 2006;8:485–91.
30. Boulter E, Garcia-Mata R, Guilluy C, Dubash A, Rossi G, Brennwald PJ, et al. Regulation of RHO GTPase crosstalk, degradation and activity by RHOGDI1. Nat Cell Biol 2010;12:477–83.
31. Su L, Agati JM, Parsons SJ. p190RHOGAP is cell cycle regulated and affects cytokinesis. J Cell Biol 2003;163:571–82.
32. Lynch EA, Stall J, Schmidt G, Chavrier P, D'Souza-Schorey C. Proteasome-mediated degradation of Rac1-GTP during epithelial cell scattering. Mol Biol Cell 2006;17:2236–42.
33. Johansen T, Lamark T. Selective autophagy mediated by autophagic adapter proteins. Autophagy 2011;7:279–96.
34. Linares JF, Amanchy R, Greis K, Diaz-Meco MT, Moscat J. Phosphorylation of p62 by cdk1 controls the timely transit of cells through mitosis and tumor cell proliferation. Mol Cell Biol 2011;31: 105–17.
35. Kadandale P, Stender JD, Glass CK, Kiger AA. Conserved role for autophagy in RHO1-mediated cortical remodeling and blood cell recruitment. Proc Natl Acad Sci U S A 2010;107:10502–7.
36. Mathew R, Karp CM, Beaudoin B, Vuong N, Chen G, Chen HY, et al. Autophagy suppresses tumorigenesis through elimination of p62. Cell 2009;137:1062–75.
37. Duran A, Linares JF, Galvez AS, Wikenheiser K, Flores JM, Diaz-Meco MT, et al. The signaling adaptor p62 is an important NF-kappaB mediator in tumorigenesis. Cancer Cell 2008;13:343–54.
38. Inami Y, Waguri S, Sakamoto A, Kouno T, Nakada K, Hino O, et al. Persistent activation of Nrf2 through p62 in hepatocellular carcinoma cells. J Cell Biol 2011;193:275–84.
39. Pohl C, Jentsch S. Midbody ring disposal by autophagy is a post-abscission event of cytokinesis. Nat Cell Biol 2009;11:65–70.
40. Kuo TC, Chen CT, Baron D, Onder TT, Loewer S, Almeida S, et al. Midbody accumulation through evasion of autophagy contributes to cellular reprogramming and tumorigenicity. Nat Cell Biol 2011;13: 1214–23.
41. Sagona AP, Nezis IP, Pedersen NM, Liestøl K, Poulton J, Rusten TE, et al. PtdIns(3)P controls cytokinesis through KIF13A-mediated recruitment of FYVE-CENT to the midbody. Nat Cell Biol 2010;12: 362–71.
42. Piekny A, Werner M, Glotzer M. Cytokinesis: welcome to the RHO zone. Trends Cell Biol 2005;15:651–8.
43. Yüce O, Piekny A, Glotzer M. An ECT2-centralspindlin complex regulates the localization and function of RHOA. J Cell Biol 2005;170: 571–82.
44. Miller AL, Bement WM. Regulation of cytokinesis by RHO GTPase flux. Nat Cell Biol 2009;11:71–7.
45. Chan CH, Lee SW, Li CF, Wang J, Yang WL, Wu CY, et al. Deciphering the transcriptional complex critical for RHOA gene expression and cancer metastasis. Nat Cell Biol 2010;12:457–67.
46. Kerscher O, Felberbaum R, Hochstrasser M. Modification of proteins by ubiquitin and ubiquitin-like proteins. Annu Rev Cell Dev Biol 2006;22:159–80.
47. Sahai E, Marshall CJ. RHO-GTPases and cancer. Nat Rev Cancer 2002;2:133–42.
48. Perez-Sala D, Boya P, Ramos I, Herrera M, Stamatakis K. The C-terminal sequence of RHOB directs protein degradation through an endo-lysosomal pathway. PLoS One 2009;4:e8117.
49. Schmidt-Mende J, Geering B, Yousefi S, Simon HU. Lysosomal degradation of RHOH protein upon antigen receptor activation in T but not B cells. Eur J Immunol 2009;40:525–9.
50. Cetin S, Ford HR, Sysko LR, Agarwal C, Wang J, Neal MD, et al. Endotoxin inhibits intestinal epithelial restitution through activation of RHO-GTPase and increased focal adhesions. J Biol Chem 2004;279: 24592–600.